J Fail. Anal. and Preven. (2022) 22:2147–2153
https://doi.org/10.1007/s11668-022-01530-6

CASE HISTORY—PEER-REVIEWED

Microstructural Aspects of Premature Pitting Corrosion of Steel Pipe–Case Study

Dorota Tyrała · Bogdan Pawłowski

Submitted: 22 October 2022 / Accepted: 27 October 2022 / Published online: 8 November 2022

Abstract A premature pitting corrosion in seam-welded 3-inch L235 steel pipe was reported to occur after 8 years in service. This pipe was part of a closed ice water cooling system, where the inlet water temperature was 6 °C and the outlet water temperature was 11 °C. The present work aimed to investigate the causes of this premature pitting corrosion of the pipe through metallographic investigations. This work comprised a visual examination of the internal surfaces of the pipe and microstructural examinations of the corrosion perforation regions (pitting corrosion areas) using optical and scanning electron microscopy (SEM) with energy dispersive X-ray (EDX) analysis. The investigations showed that the corrosion pits occurred only in areas with a huge number of specific micro-voids that can be associated with the excessive presence of trapped hydrogen dissolved in the steel, probably during steelmaking operations.

Keywords Ice water cooling system · Seam-welded steel pipes · Pitting corrosion · Trapped hydrogen

Introduction

Iron and steel pipes have been used in water distribution or cooling systems for over five centuries [1]. However, a huge number of cases of corrosion of steel pipes in such systems can be found in the literature, e.g., [2–11]. A very common cause of failures has been local leaks resulting from pitting corrosion caused by various factors. Internal pitting corrosion is a significant factor in the degradation of pipelines. Pipe failure can occur if a pit fully penetrates the pipe wall. Both carbon steel and corrosion-resistant alloys can undergo pitting corrosion. The susceptibility of metals to pitting corrosion and the pitting corrosion rate depend on the metallurgy of the metal and the environment in which it is operating [12, 13].

Anode formation is a prerequisite for pitting corrosion. The formation of an anode can be caused mainly by heterogeneity of the metal surface layer (the presence of grain boundaries, impurities, cracks, roughness, etc.), breakdown of the passive film and deposition of solid particles on the metal surface, which leads to the formation of anode and cathode areas [14, 15].

Overall, it can be said that for a defect-free "perfect" material, pitting corrosion is caused by an environment (chemistry) that may contain aggressive chemical species such as chloride. For a homogeneous environment, pitting is caused by a material that may contain inclusions (MnS is the major culprit for the initiation of pitting in steels) or defects. In most cases, both the environment and the material contribute to pitting initiation.

The purpose of this work was to determine the reasons for premature pitting corrosion failure (leakage of coolant occurred at several points) in a seam-welded 3-inch L235 steel pipe, which was reported to occur after 8 years in service (Fig. 1).

This pipe was part of the closed ice water cooling system where the inlet water temperature was 6 °C and the outlet water temperature was 11 °C. According to the provided information, the flowing water contained corrosion inhibitors dedicated to closed cooling systems made of

D. Tyrała (✉) · B. Pawłowski
Faculty of Metal Engineering and Industrial Computer Science, AGH University of Science and Technology, Kraków, Al. Mickiewicza, Poland
e-mail: bpawlow@agh.edu.pl

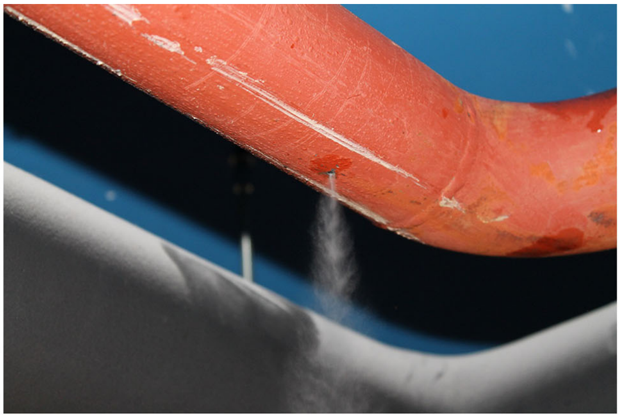

(a)

(b)

Fig. 1 Pitting failure of the pipeline (**a**) and fragment of pipe taken for testing (**b**)

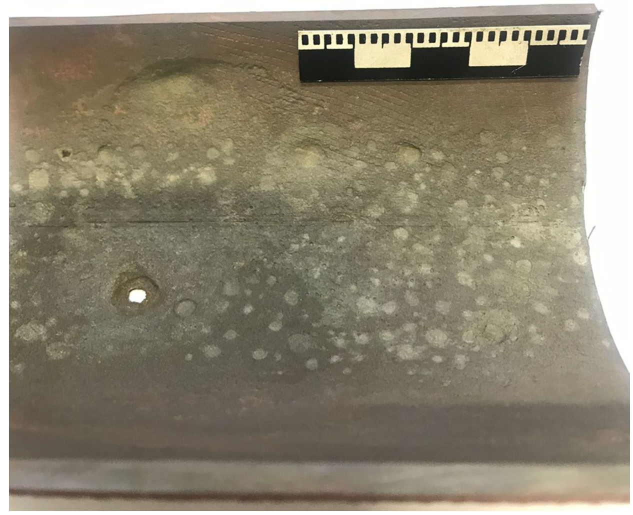

Fig. 2 Macroscopic view of the pitting area (inner surface after corrosion deposits were removed)

Table 1 The chemical composition of the examined steel

Element	L235 steel composition according to the EN 10,224:2004, wt.%	Analysis, wt.% (mass spectrometer
C	Max. 0.16	0.07
Si	Max. 0.35	0.007
Mn	Max. 1.20	0.23
P	Max. 0.030	0.015
S	Max. 0.025	0.003
Cr	…	0.01
Mo	…	< 0.005
Ni	…	< 0.005
Al	…	0.04
Cu	…	0.006
Nb	…	< 0.002
Ti	…	< 0.002
V	…	< 0.002

non-coated steels (corrosion inhibitors with the addition of non-oxidizing biocide). Flowing medium parameters such as temperature, flow rate, and chemical composition of the water were monitored, and they were within the required range.

Therefore, the main task of this work was to check whether the pipe material was responsible for the failure.

Experimental

A sample was cut from the tube, including the perforation site and the surrounding area, as presented in Fig. 2. The chemical composition of the steel from which the pipe was made was checked. Mass spectrometer Foundry Master was applied to the determination of the chemical composition.

Microstructure analyses were carried out with a light optical microscope (LOM), Zeiss Axiovert 200 MAT, and by a scanning electron microscopy, FEI INSPECT S50, with microanalysis by energy dispersive spectroscopy (EDS) for analysis of corrosion deposits.

Metallographic examinations were performed on specimens etched with 2% nital (nitric acid in ethanol).

Results and Discussion

As it can be seen from the data presented in Table 1, the chemical composition of the examined steel complied with the requirements of the relevant standard.

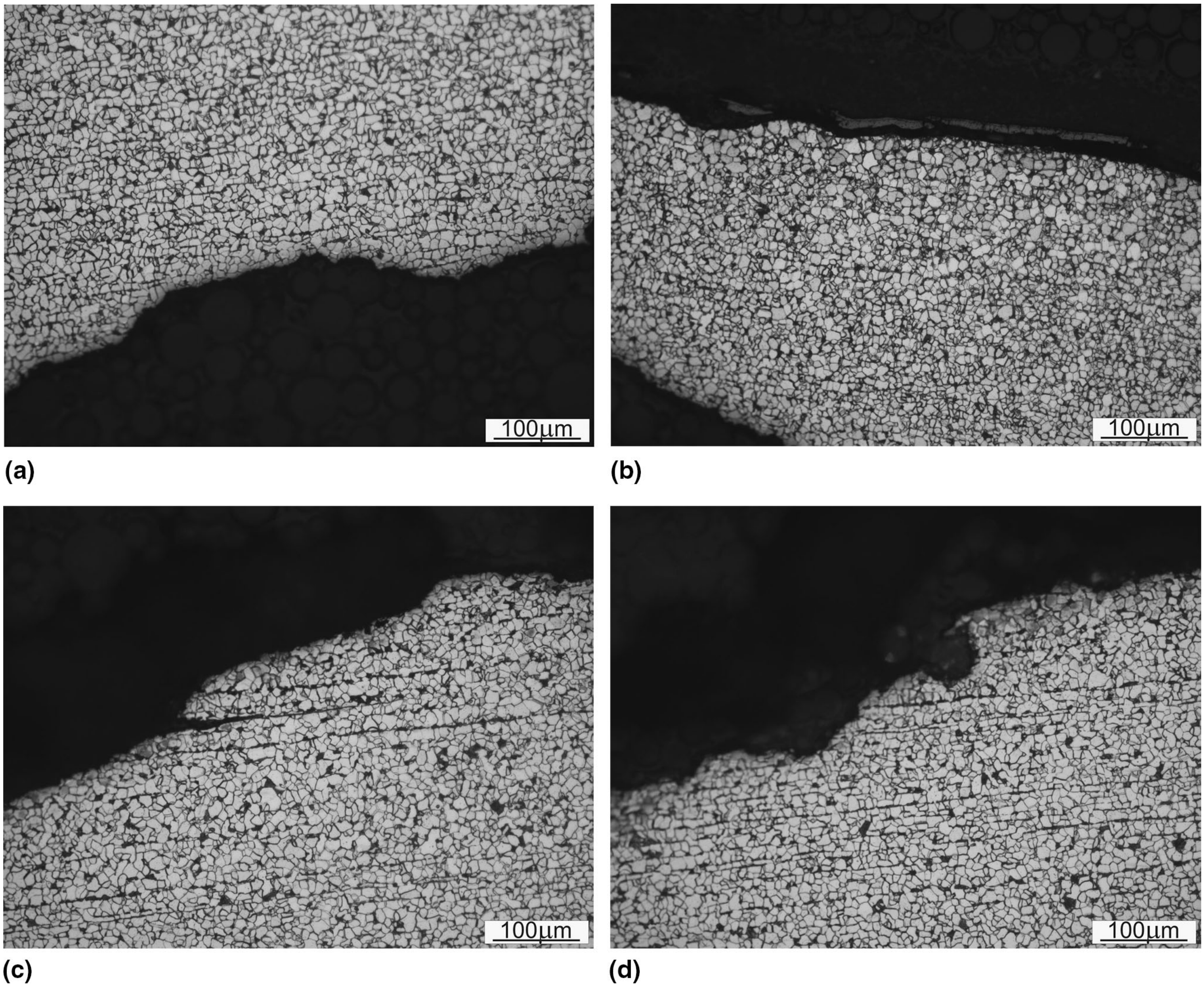

Fig. 3 Microstructures near the corrosive perforation, both transverse (**a**, **b**) and longitudinal (**c**, **d**) cross section

Visual examination of the internal surfaces of the pipe near the perforation revealed that there were many corrosion pits of larger and smaller sizes that did not perforate the pipe wall (Fig. 2). This photograph also shows the seam weld line is not the preferred pitting site. It is worth noting that the inner surface of the pipe away from the perforation was free of pitting.

Metallographic examinations revealed a typical microstructure for this type of steel, consisting of ferrite grains with small islands of perlite. Typical microstructures are shown in Fig. 3.

Apart from the perlite grains (in the photographs of dark areas) arranged most often in bands alternating with bright ferrite grains, several dark areas were also observed which could not be clearly identified in the light microscope.

Nothing was observed during the metallographic examinations that could explain the pitting corrosion and perforation of the pipe wall. Therefore, further observations of the microstructure were made using scanning electron microscopy.

EDS analysis of sediments collected from inside the pipe showed that they are only corrosion products (iron oxides), as shown in Fig. 4.

SEM observations of microstructures near the corrosive perforation revealed the presence of three types of microscopic defects. Examples of defects of the first type are in the form of regular voids (micropores), as shown in Fig. 5.

The second type of observed defects are microcracks, mainly at the grain boundaries–Fig. 6

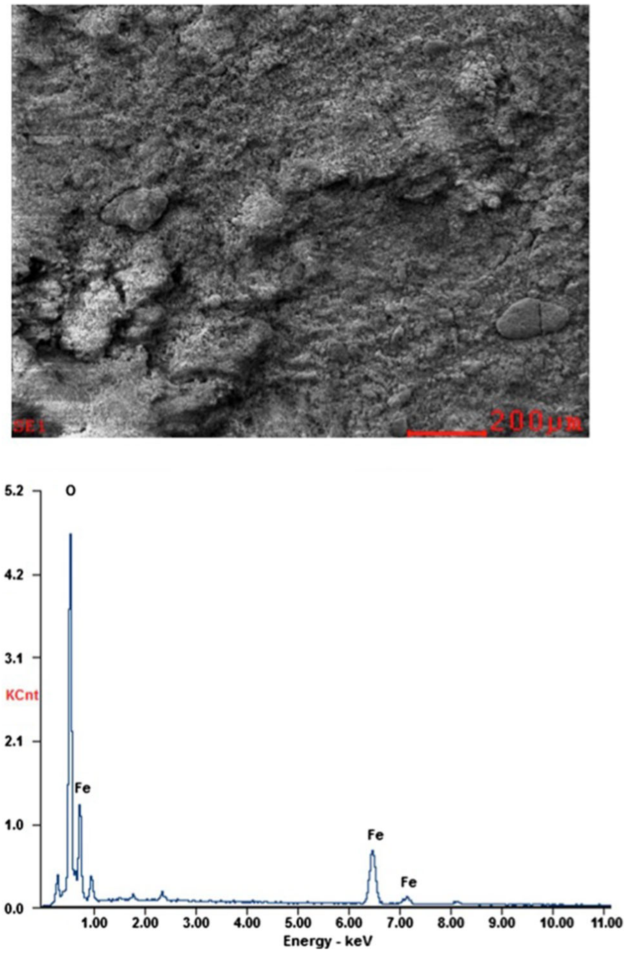

Fig. 4 EDS area analysis of sediments collected from inside the pipe

The third type (so-called "rooster feet") was most often observed in the form of local deformation areas at the bottom of which microcracks were visible, as shown in Fig. 7.

According to the diagram (Fig. 8) presented in an extensive study by the Graz University of Technology [16], the microstructure defects observed in this study are probably caused by the presence of dissolved hydrogen in the steel.

In fact, Rossmann's diagram is a modification of the scheme presented by Engel and Klingele forty-five years ago [17, 18].

It is known that steel may pick up hydrogen via many different routes, for example, during the steelmaking process and heat treatment process or steel sheet pickling, and this is inevitably deleterious to the metal [19].

Hydrogen can be easily captured at hydrogen trapping sites during its diffusion into the material, and then it

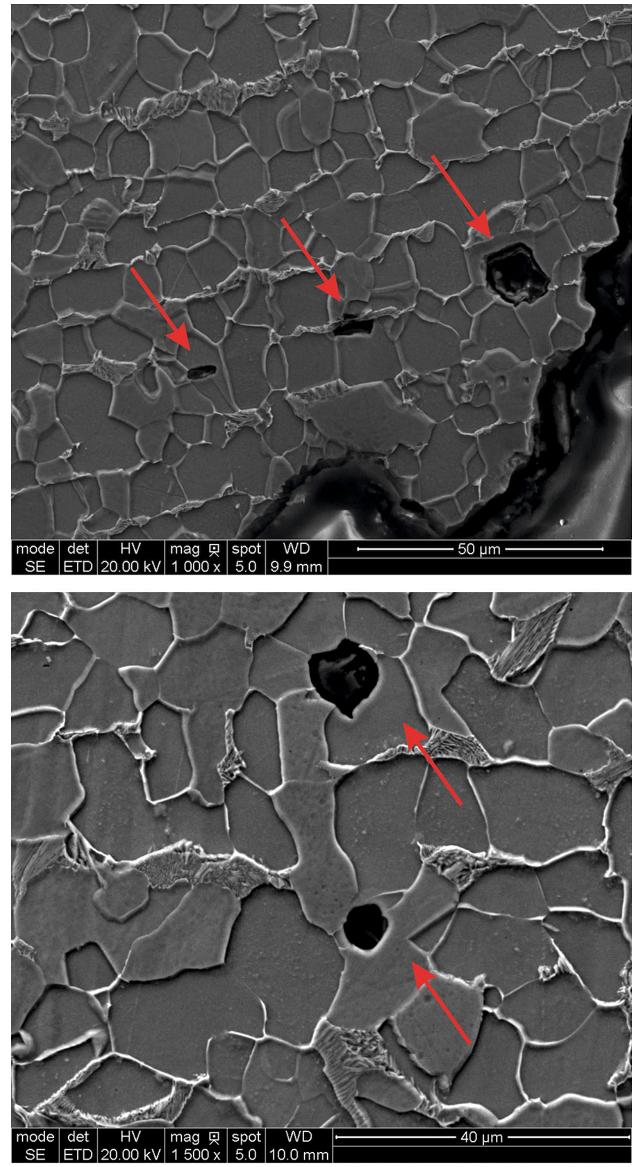

Fig. 5 Micro-voids (micropores)–the first type of observed microdefects

accumulates at voids or defects within the steel, forming molecular hydrogen (Fig. 9). The molecular hydrogen leads to an inner pressure increment and microcrack initiation which consequently accelerates the pitting corrosion processes [20].

Conclusions

The following conclusions can be drawn from the presented study:

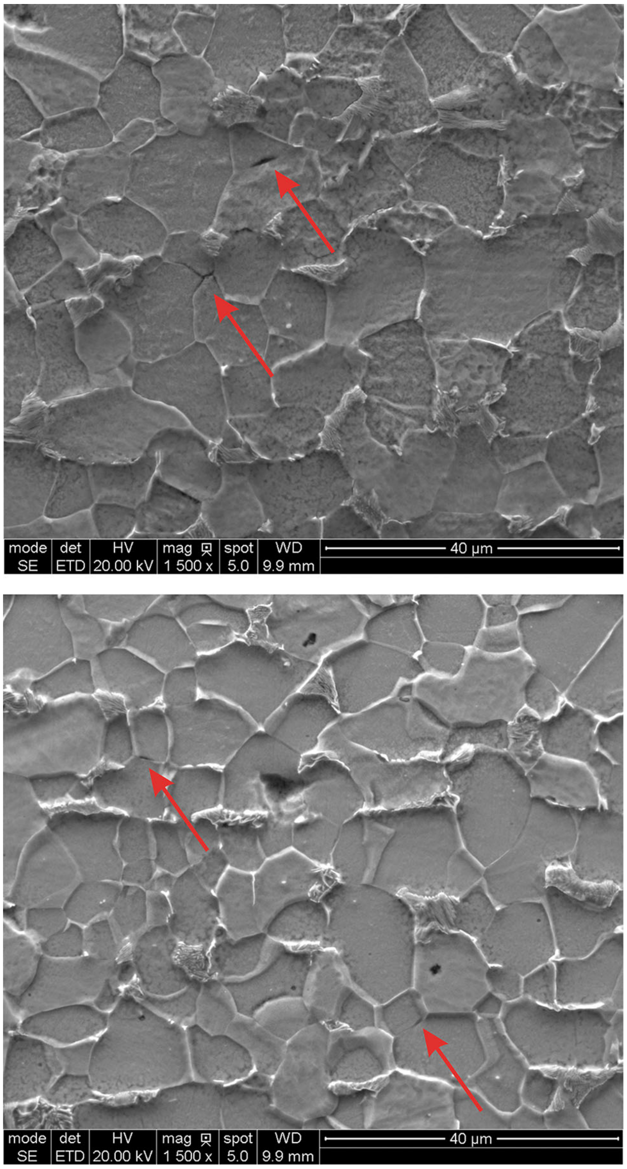

Fig. 6 Microcracks–the second type of observed microdefects

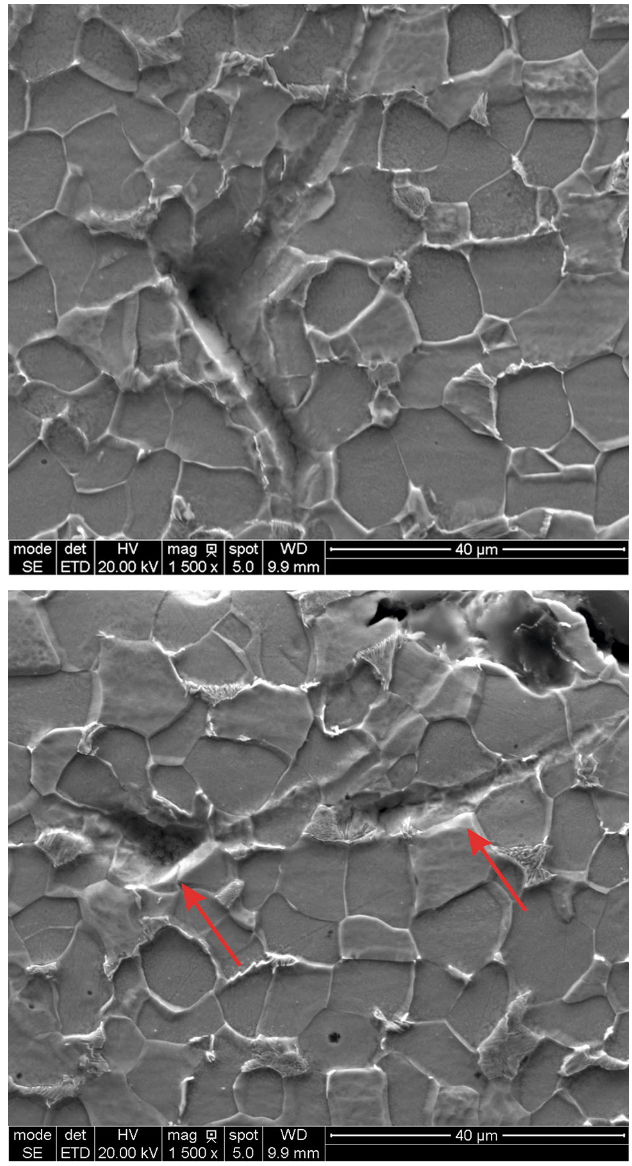

Fig. 7 Local deformation areas–third type of observed microdefects

- Near the pipe perforation site, there were many corrosion pits of larger and smaller sizes, yet they did not perforate the pipe wall.
- The seam weld line is not the preferred pitting site.
- The inner surface of the pipe away from the perforation was free of pitting.
- SEM observations of microstructures near the corrosive perforation revealed the presence of many microscopic defects (only in the pitting area).
- According to the diagram presented in an extensive study by the Graz University of Technology (Axel Rossmann, Aeroengine Safety, Graz University of Technology 2020), the microstructure defects observed in this study are likely associated with the presence of trapped hydrogen.
- Many microstructure defects in the steel pipe strongly accelerate the pitting corrosion processes in the ice

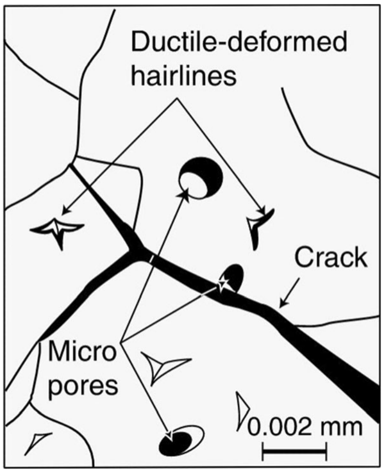

Fig. 8 The microstructure defects caused by hydrogen (scheme by Axel Rossmann)

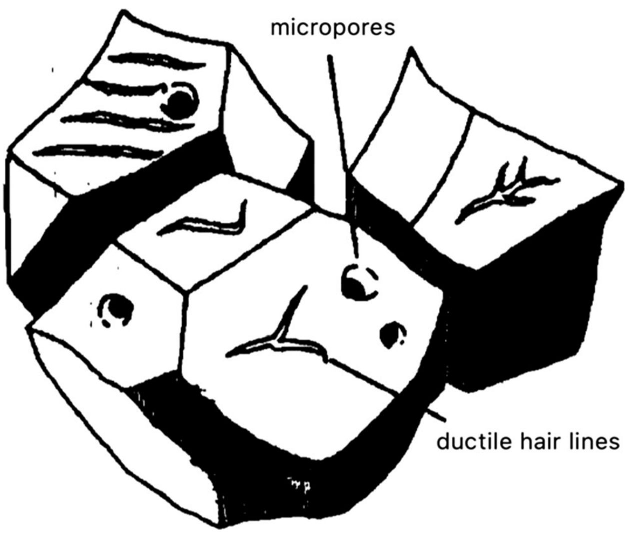

Fig. 9 The microstructure defects caused by hydrogen (scheme by Engel and Klingele)

water environment, despite the addition of corrosion inhibitors.

References

1. L.S. McNeill, M. Edwards, Iron pipe corrosion in distribution systems. J. Am. Water Works Assoc. **93**(7), 88–100 (2001)
2. M. Edwards, Controlling corrosion in drinking water distribution systems: a great challenge for the 21st century. Water Sci. Technol. **9**(2), 1–8 (2004)
3. D.F. Shams, S. Islam, B. Shi, W. Khan, B. Gunawardana, M. Saad, M. Qasim, H.A. Javed, S.G. Afridi, M. Naeem, G.S. Khan, Characteristics of pipe corrosion scales in untreated water distribution system and effect of water quality in Peshawar. Pakistan. Environ. Sci. Pollut. Res. **26**(6), 5794–5803 (2019)
4. F. Delaunois, F. Tosar, V. Vitry, Corrosion behaviour and biocorrosion of galvanized steel water distribution systems. Bioelectrochemistry. **97**(2014), 110–119 (2014)
5. C.A. Della Rovere, R. Silva, C. Moretti, S.E. Kuri, Corrosion failure analysis of galvanized steel pipes in a water irrigation system. Eng. Fail. Anal. **33**, 381–386 (2013)
6. B. Pawlowski, D. Tyrala, M. Pilch, Metallographic investigations of the premature corrosion failure of steel seam-welded galvanized cold water pipes. J. Fail. Anal. Prev. **20**(3), 9–14 (2020)
7. K. Slavíčková, A. Grünwald, B. Šťastný, Monitoring of the corrosion of pipes used for the drinking water treatment and supply. Civ. Eng. Architect. **1**, 61–65 (2013)
8. J. Lin, M. Ellaway, R. Adrien, Study of corrosion material accumulated on the inner wall of steel water pipe. Corros. Sci. **43**(11), 2065–2081 (2001)
9. P. Sarin, V.L. Snoeyink, J. Bebee, K.K. Jim, M.A. Beckett, W.M. Kriven, J.A. Clement, Iron release from corroded iron pipes in drinking water distribution systems: effect of dissolved oxygen. Water Res. **38**(5), 1259–1269 (2004)
10. A. Colombo, L. Oldani, S.P. Trasatti, Corrosion failure analysis of galvanized steel pipes in a closed water cooling system. Eng. Fail. Anal. **84**, 46–58 (2018)
11. D. Tyrala, B. Pawlowski, Failure analysis of premature corrosion of HF seam-welded steel pipe in central heating system. J. Fail. Anal. Prev. **21**(3), 772–778 (2021)
12. P. Sarin, V.L. Snoeyink, J. Bebee, W.M. Kriven, J.A. Clement, Physico-chemical characteristic of corrosion scales in old iron pipes. Water Res. **35**(12), 2961–2969 (2001)
13. S. Papavinasam, *Pitting corrosion, trends in oil and gas corrosion research and technologies* (Woodhead Publishing Series in Energy, New York, 2017), p. 663–688
14. K.V. Akpanyung, R.T. Loto, Pitting corrosion evaluation: a review. J. Phys: Conf. Ser. **1378**, 022088 (2019)
15. G.T. Burstein, C. Liu, R.M. Souto, S.P. Vines, Origins of pitting corrosion, corrosion engineering, science and technology, the international journal of corrosion processes and corrosion. Control. **39**(1), 25–30 (2004)
16. https://aeroenginesafety.tugraz.at/lib/exe/fetch.php?media=:5:54:544:effects-of-hydrogen-on-the-structure.svg
17. L. Engel, H. Klingele, Beitrag des Rasterelektronenmikroskops zur Beurteilung wasserstoffinduzierter Brüche. Period. Arch. Eisenhütt. **48**(10), 555–560 (1977)
18. L. Engel, H. Klingele, *Atlas of metal damage* (Prentice Hall, New York, 1981), p. 125
19. H.C. Ma, D. Zagidulin, M. Goldman, D.W. Shoesmith, Influence of iron oxides and calcareous deposits on the hydrogen permeation rate in X65 steel in a simulated groundwater. Int. J. Hydrogen Energy. **46**, 6669–6679 (2021)
20. L. Li, M. Mahmoodian, C.-Q. Li, D. Robert, Effect of corrosion and hydrogen embrittlement on microstructure and mechanical properties of mild steel. Constr. Build. Mater. **170**, 78–90 (2018)